Characterization of Ionic Clusters in Different Ionically Functionalized Diblock Copolymers by CW EPR and Four-Pulse Double Electron−Electron Resonance

M. Pannier, M. Schöps, V. Schädler, U. Wiesner,† G. Jeschke, and H. W. Spiess*

Max-Planck-Institut für Polymerforschung, Postfach 3148, D-55021 Mainz, Germany

Received January 30, 2001

ABSTRACT: The size of ion clusters, distances between them, and the dynamics of their environment in ionically functionalized diblock copolymers were characterized by variable temperature continuous-wave electron paramagnetic resonance (CW EPR) and pulse double electron−electron resonance (DEER). CW EPR on ionic spin probes attached to the clusters reveals whether they are situated in the block copolymer interface and provides semiquantitative information on the fraction of cluster surface exposed to the polystyrene or polyisoprene microphase. DEER measurements show that ion cluster sizes do not depend on the topology of the ionomer and on chain length. For α,*ω*-macrozwitterionic block copolymers, where the clusters exhibit a two-dimensional distribution in the block copolymer interface, intercluster distances also do not depend on chain length. For monoionic species the intercluster distance obeys a $^1/_3$ scaling law with respect to the molecular mass of the polymer, suggesting constant polymer density and an unchanging spatial arrangement of the clusters.

Introduction

Self-assembly of molecules is one of nature's most important ways to build highly functional nanoscale structures as they are found in living organisms.[1] As this principle allows for a high degree of control by fine-tuning the constituent molecules but does not involve a tedious step-by-step synthesis of the whole structure, it is also very attractive in materials science.[2] By combining the self-organization behavior of ionomers[3,4] with that of block copolymers,[5−7] we were able to generate a series of polymer structures with well-defined features on nanoscopic length scales.[8−10] These structures are distinguished by the possibility to tune characteristic length scales or even to switch microdomain morphology by addition of low molecular weight salts. The characterization of both dynamics and nanostructure of these ionomers required the use of advanced electron paramagnetic resonance (EPR) probe techniques.[9,11]

In the present work we use such techniques to localize the ionic aggregates in the recently described *μ*,*ω*-macrozwitterionic diblock copolymers, where the ionic clusters located in the interface between the blocks are of crucial influence for determining the morphology.[10] Moreover, we investigate systematically the dependence of ion cluster sizes and intercluster distances on the polymer chain length in α,*ω*-macrozwitterionic and monoionic diblock copolymers. Finally, we compare cluster sizes and intercluster distances in α,*ω*- and *μ*,*ω*-macrozwitterionic diblock copolymers with similar chain lengths. The results provide insight into how the curvature of the block copolymer interface influences the dynamics close to the ion cluster surface and allow us to check our earlier conjectures on the location of the ion clusters with respect to the block copolymer interface.

† Present address: Materials Science & Engineering, Cornell University, 329 Bard Hall, Ithaca, NY 14853-1501.

Experimental Section

Sample Preparation and Characterization. α,*ω*-Macrozwitterionic poly(styrene-*block*-isoprene) diblock copolymers were prepared by anionic polymerization and subsequent introduction of the ionic end groups,[8,12] and *μ*,*ω*-macrozwitterionic and -monoionic poly(styrene-*block*-isoprene) (PS−PI) diblock copolymers were prepared by anionic polymerization using 1-(4′-(*N*,*N*-dimethylamino)methylphenyl)-1-phenylethene (MDPE) as monomer between the blocks and subsequent quaternization of the tertiary amino group.[13] All samples with a given molecular weight but different end groups were derived from the same polymerization batch, thus ensuring identical molecular weight distributions and stereochemistry of the polyisoprene chain. Sample characterization has been described elsewhere.[8−10,13] Small-angle X-ray scattering (SAXS) and transmission electron microscopy (TEM) were used to determine the morphology of the samples. The spin probe 4-carboxy-TEMPO was converted to its potassium salt (K-TEMPO) by titration with 0.1 mM methanolic KOH. The samples for EPR studies were prepared by solvent casting: 100 mg of the polymer were dissolved in 10 mL of toluene and mixed with the calculated amount of 0.05% methanolic spin probe solution such that the ratio of spin probes per ionic chain ends was 2/15. After film casting and solvent evaporation the samples were dried and annealed under vacuum at 120 °C for more than 6 h, before being transferred to the EPR tube. The ionomers studied in this work are shown in a schematic representation in Figure 1 together with the structure of the spin probe. The molecular characteristics are given in Table 1.

EPR Spectroscopy. EPR spectra and DEER traces were measured at a Bruker ESP 380E pulse EPR spectrometer (X-band, ca. 9.7 GHz) equipped with a rectangular cavity for continuous-wave (CW) EPR and an ENDOR probehead EN 4118X-MD-4 (Bruker) for DEER. Variable-temperature CW EPR was performed using a Bruker ER 4111 VT temperature control unit and employing a modulation amplitude of 0.02 mT and a MW power of 6.3 mW. For DEER, the ENDOR resonator was overcoupled to $Q_L \approx 100$ to provide for a bandwidth sufficient for the double-resonance experiment. Microwave from an external tunable second microwave source (Avantek AV 78012 YIG oscillator customized by Magnettech GmbH, Berlin) was fed to one MW pulse former unit of the spectrometer. All DEER measurements were performed with

10.1021/ma010169c CCC: $20.00
Published on Web 07/03/2001

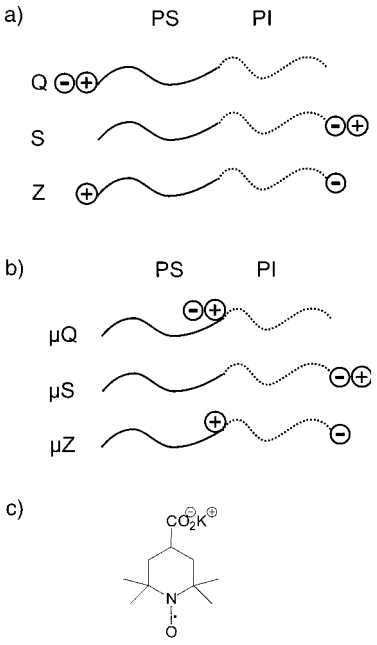

Figure 1. Schematic representation of the investigated ionomers and the spin probe: (a) α,ω-type ionomers; (b) μ,ω-type ionomers; (c) potassium salt of 4-carboxy-2,2,6,6-tetramethylpiperidine-1-oxyl (K-TEMPO).

Table 1. Molecular Characteristics of the Investigated Polymers

sample	S11, Z11	S17, Z17	S24, Z24	S49, Z49	μS25, μQ25, μZ25
M_n [kg/mol]	11.0	16.5	24.0	49.0	25.3
M_n(PS) [kg/mol]	5.9	8.5	12.7	25.0	11.7
M_w/M_n	1.13	1.10	1.09	1.08	1.05
1,4-PI [mol %]	28	27	29	28	45

liquid helium cooling at a temperature of 15 K at repetition rates of 100 Hz with pulse lengths of 32 ns for all microwave pulses and a difference between pump and observer frequency of 50−70 MHz. The pump position was chosen at the maximum of the nitroxide EPR spectrum.[14]

Results and Discussion

Localization of Ion Clusters in μ,ω-Macrozwitterionic and Monoionic Block Copolymers. Stimulated by the fine-tuning of the lamellar spacing of α,ω-macrozwitterionic diblock copolymers with salt (sample Z in Figure 1a),[15] we synthesized polymers with a new ionic functionalization pattern: μ,ω-macrozwitterionic diblock copolymers.[13] The three different functionalized samples which could be derived from one batch are shown schematically in Figure 1b. On a zwitterionic μZ sample with molecular weight of 48 kg mol^{-1} we observed switching of the microdomain morphology from hexagonally packed PS cylinders in a PI matrix for a salt-free sample to the lamellar phase in a sample containing 6 equiv of salt per chain.[10] In the following we restrict the discussion to salt-free samples with a molecular weight of 25.3 kg mol^{-1} which are distinguished by sulfonate end groups (μS25), a quaternary ammonium group at the block junction (μQ25), or the combination of both these ionic groups in a macrozwitterion (μZ25). SAXS and TEM investigations revealed a lamellar morphology of the samples μS25 and μQ25.[16] In contrast, the macrozwitterionic sample μZ25 exhibits a cubic bicontinuous morphology, which may tentatively be assigned as a gyroid morphology,[17] due to a changed chain conformation which is in turn induced by ion aggregation as discussed in ref 10.

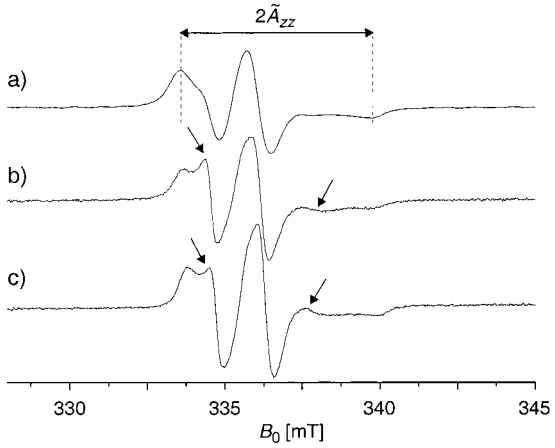

Figure 2. CW EPR spectra of K-TEMPO in three ionomers (see Figure 1 and Table 1) at 340 K: (a) μS25; the definition of the maximum extrema separation $2\tilde{A}_{zz}$ is indicated. (b) μQ25; features due to the more mobile component are marked by arrows. (c) μZ25; features due to the more mobile component are marked by arrows.

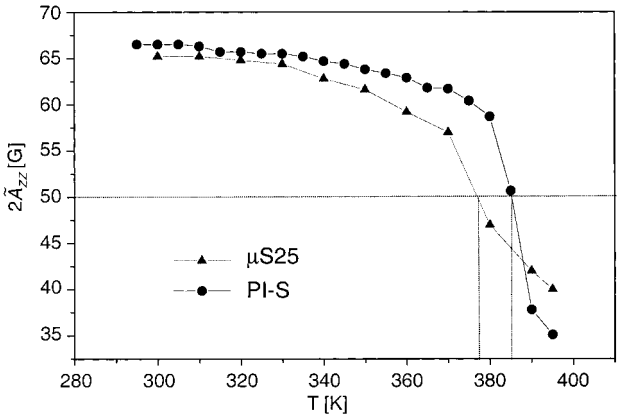

Figure 3. Temperature dependence of the maximum extrema separation $2\tilde{A}_{zz}$ for sample μS25 (triangles) and sample PI−S from ref 8 (circles).

Variable-temperature CW EPR studies, as described for the α,ω-macrozwitterionic diblock copolymers,[9] were performed to localize the ion aggregates. The spectrum of sample μS25 (Figure 2a) corresponds to a monomodal distribution of rotational correlation times and can conveniently be characterized by the maximum extrema separation $2\tilde{A}_{zz}$. With increasing temperature the inverse rotational correlation time of the nitroxide probe molecule approaches the anisotropy of the hyperfine interaction, which is thus partially averaged. The dynamic process can therefore be characterized by the temperature T'_{50G} corresponding to an extrema separation of 50 G (5 mT) and to the most pronounced change in $2\tilde{A}_{zz}$. Note that T'_{50G} is related to the mobility of the ionic spin probes attached to the ionic clusters,[8] rather than to the polymer chain dynamics as the more common T_{50G}.[18,19] The latter characteristic temperature can be measured with nonpolar spin probes in our polymers and is significantly lower.[8,16] As can be seen in Figure 3, the temperature dependence of $2\tilde{A}_{zz}$ for sample μS25 with $T'_{50G} = 377$ K is quite similar as for sample PI−S from ref 8 with $T'_{50G} = 385$ K. Indeed, this similarity is anticipated since the lithium sulfonate aggregates are expected to form in the PI matrix in both samples. The fact that the T'_{50G} values are about 100 K

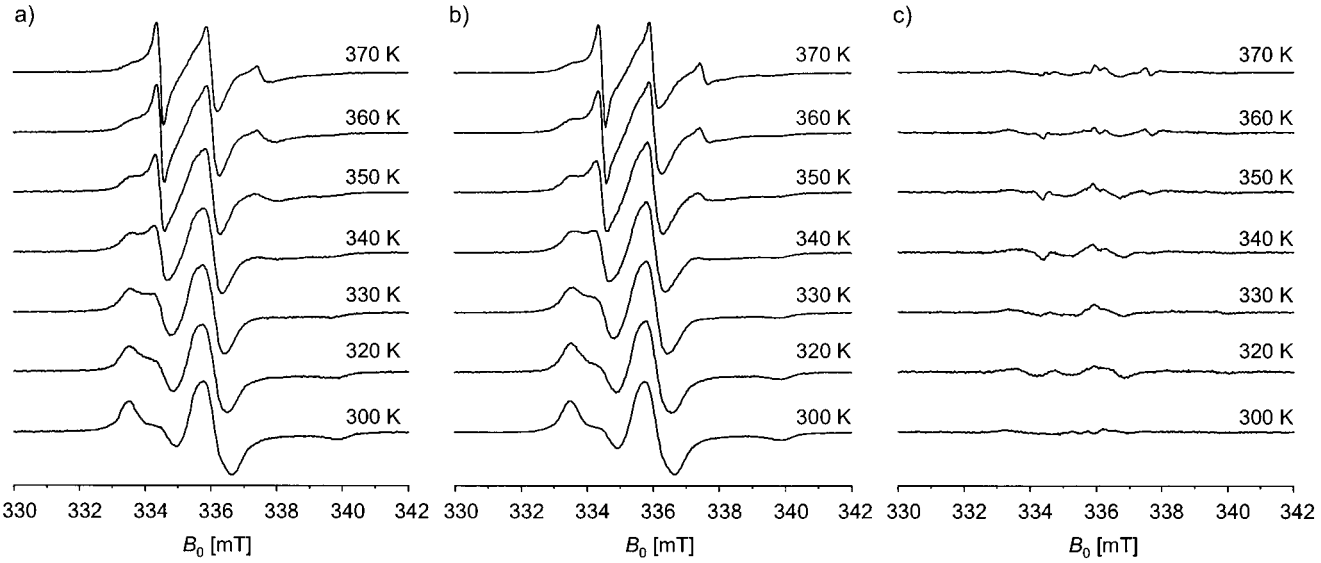

Figure 4. Comparison of experimental CW EPR spectra of μQ25 (a) with spectra simulated by a weighted superposition of the spectra of μS25 and PI-Q at the same temperature (b). The normalized weighting factor for the slow component (μS25) is 0.70 ± 0.05 throughout the displayed temperature range. (c) Fit residuals.

above the glass transition temperature of the PI block proves that the spin probe is attached to the ion cluster. The difference $T'_{50G} = 8$ K between the two samples can be attributed to the slightly higher 3,4-PI content in sample PI−S which causes a decrease in chain mobility and a glass transition temperature that is 19 K higher than for the PI block in μS25. Lithium sulfonate aggregates in a PS matrix ($T'_{50G} = 430$ K)[8] can be safely excluded.

For sample μQ25 with functionalization at the block junction point (see Figure 1b) the CW EPR spectrum corresponds to a bimodal distribution of rotational correlation times as can be seen clearly in Figure 2b where features due to the component with higher mobility are marked by arrows. We have observed such bimodal spectra before in an α,ω-macrozwitterionic diblock copolymer and attributed them to a localization of the ion clusters in the diblock copolymer interface where the dynamic environment of the spin probes is heterogeneous.[9] This previous interpretation is fully supported by the new results for μQ25 and μZ25 (Figure 2c) for which the chemical structure enforces the localization of the ion clusters in the interface region.

A quantification of the more mobile and the more rigid contribution to the bimodal distribution of correlation times is possible by simulating the CW EPR spectra as a numerical superposition of reference spectra for the two dynamical components.[9] We have simplified the model from ref 9 by eliminating the third, highly mobile component and by requiring that both reference spectra are taken at the same temperature as the experimental spectrum. The simplified analysis is based on the equation

$$I_{\mu Q25}(T) = w_1 I_{\mu S25}(T) + w_2 I_{PI-Q}(T) \qquad (1)$$

where $I_{\mu Q25}$, $I_{\mu S25}$, and $I_{\mu PI-Q}$ are the spectral line shape functions of the samples μQ25, μS25, and PI-Q from ref 8, and w_1 and w_2 are weighting factors for the "slow" and "fast" component, respectively, with the normalization condition $w_1 + w_2 = 1$. The number of free parameters per spectrum is thus reduced to one, yet the least-squares fits are of similar quality as with the earlier, more elaborate model, as can be seen in Figure 4. We wish to emphasize that the reference spectra of μS25 and PI-Q only serve as close fits of the line shape of the "slow" and "fast" component in the spectra of μQ25; it is not warranted to conclude that the chemical environments of the spin probes are the same for the components and their respective reference spectra. Throughout the temperature range from 300 to 370 K, where the most dramatic line shape changes are observed, the best fits are obtained with $w_1 = 0.70 \pm 0.05$. No systematic trend in this parameter is observed.

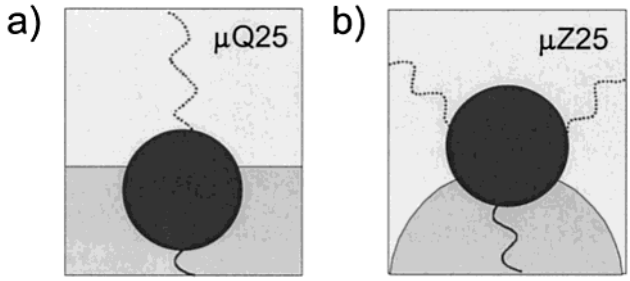

Figure 5. Schematic drawing of the cluster location in μQ25 (a) and μZ25 (b).

Significantly, the spectra of the sample μZ25 in the same temperature range can be fitted with the same model and reference spectra (data not shown), but in this case we obtain $w_1 = 0.28 \pm 0.04$. In a simplified picture, where the boundaries between the ion cluster and the polymer and between the two polymer microphases are sharply defined, this can be interpreted as clusters with a larger part of their surface exposed to the more rigid PS microphase in the sample μQ25 and clusters with a larger part of the surface exposed to the more mobile PI microphase in the sample μZ25. For μQ25 with lamellar morphology this implies a slightly higher preference of the cluster for the PS phase (Figure 5a), while the trend from μQ25 to μZ25 is expected due to the morphology change from a lamellar to a cubic bicontinuous structure (Figure 5b). The curvature of the PI−PS interface, which causes the higher exposure of the cluster surface to PI, resembles the situation in a I_2S miktoarm star copolymer.[20]

Ion Cluster Sizes and Intercluster Distances in Ionomers. Distances between the ionic clusters in

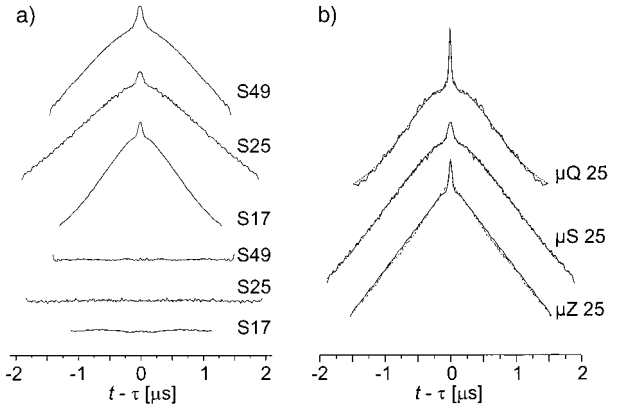

Figure 6. Ionomer DEER time-domain data and fits based on bimodal distance distributions for selected ionomers (see Figure 1 and Table 1): (a) S17, S25, and S49. Experimental data (top) and fit residuals (bottom). (b) μQ25, μS25, and μZ25. Fits are superimposed as dashed lines.

diblock copolymers are not easily obtained from SAXS since the scattering intensity due to the contrast between the polymer microphases dominates. This problem does not exist in EPR distance measurements[21,22] which make use of the high selectivity of ionic spin probes for the ion clusters. We have recently introduced DEER[14,23,24] measurements on such ionic spin probes as a characterization method which cannot only reveal the intercluster distances but also provides information on the cluster size without requiring assumptions on the cluster shape.[11] The method is based on the r^{-3} dependence of the dipole−dipole coupling between two spins localized at a distance r and does not depend on long-range order or a particular model for the distribution of the probes. Work on shape-persistent rodlike biradicals shows that DEER[25] and similar technically more simple methods[26] yield distances with a precision of 0.05−0.2 nm in the range between 2 and at least 5 nm. In the ionomer samples, distance distributions with at least two peaks corresponding to the cluster size and next-neighbor intercluster distances are expected. Since the peaks are broadened due to incomplete ordering and the distribution of spin probes on the cluster surface, a precision of about 0.5 nm is sufficient which means that a distance range up to at least 7 nm can be accessed.

In the experimental time-domain data, shown in Figure 6 for selected samples, fast decaying signals close to $t - \tau = 0$ correspond to short distances (cluster size) and longer lasting oscillations to longer distances (intercluster distance) while an exponentially decaying background signal is due to the approximately homogeneous distribution of spin pairs with distances much longer than the next-neighbor intercluster distance. The corresponding model of a distance distribution consisting of two Gaussian peaks and the homogeneous background contribution[11] fits the experimental data rather well as can be seen from the fit residuals in Figure 6a and the superimposed fits in Figure 6b. Similar data were obtained for the α,ω-macrozwitterionic diblock copolymers and for sample S11 (not shown). The parameters of the two Gaussian peaks for all the investigated polymers are given in Table 2, and the dependence of the cluster size and intercluster distance on the molecular weight of the polymers is displayed in Figure 7 for the α,ω-macrozwitterionic (squares) and monoionic, end-capped (circles) diblock copolymers. The peak widths in the distance distribution vary between

Table 2. DEER Distances (nm) of the Investigated Polymers

sample	$r_1^{\mathrm{DEER}\,a}$	$\sigma(r_1^{\mathrm{DEER}})$	$r_2^{\mathrm{DEER}\,b}$	$\sigma(r_2^{\mathrm{DEER}})$
S11	1.89	0.67	4.78	0.73
S17	1.82	0.35	5.32	0.71
S24	2.22	0.49	6.31	0.72
S49	1.88	0.36	7.67	0.76
Z11	1.85	0.45	4.76	1.33
Z17	1.91	0.40	4.97	0.77
Z24	1.95	0.59	5.03	1.22
Z49	1.96	0.49	4.91	0.81
μS25	2.22	0.49	6.31	0.72
μQ25	1.79	0.39	5.30	0.78
μZ25	1.84	0.33		

[a] Assigned to cluster size. [b] Assigned to intercluster distance.

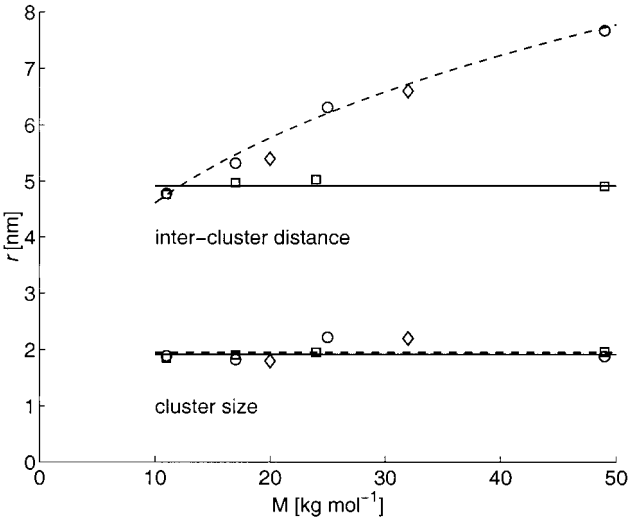

Figure 7. Dependence of cluster size and intercluster distance on the molecular weight for α,ω-macrozwitterionic (squares and full lines, samples Z11, Z17, Z25, and Z49) and monoionic (circles and dashed lines, samples S11, S17, S25, and S49) block copolymers as well as monoionic homopolymers (diamonds, samples PI-Q10 and PI-Q16 from ref 11, corresponding to block copolymer molecular weights of 20 and 36 kg mol^{-1}). The lines are fits assuming constant cluster sizes, a constant intercluster distance for the zwitterionic series, and a scaling law $r = 2.09M^{0.334}$ for the intercluster distances in the monoionic series.

0.35 and 0.7 nm for the cluster sizes in both series, between 0.7 and 0.8 nm for the intercluster distances in the monoionic series, and between 0.8 and 1.3 nm for the intercluster distances in the zwitterionic series. This variation indicates differences in the degree of ordering in the samples; significantly, the largest widths are found for samples S11 and Z11 where microphase separation is expected to be incomplete.

Given these variations in the degree of ordering, we think that the small variation of the cluster sizes seen in Figure 7 is not significant. Assuming a constant cluster size, we find average values of 1.95 nm for the zwitterionic series and 1.92 nm for the monoionic series. The cluster sizes are thus the same within experimental error, which suggests that the number of aggregating chain ends depends neither on the chain length nor on the environment of the cluster. There is also hardly a significant change in intercluster distances for the zwitterionic series; the average value is 4.92 nm. On the contrary, in the monoionic series the intercluster distance increases significantly with chain length and follows a scaling law with an exponent of 0.325. The two data points for monoionic homopolymers from our

earlier work[11] can be included in the same plot (see diamonds in Figure 7), considering that they correspond to block polymers with twice the molecular weight, which would have the same length of the poly(isoprene) block. A fit for all six points yields a scaling law $r = 2.09M^{0.334}$, with the molecular mass M given in kg mol^{-1} and the distance in nm. This result is significantly different from the square-root scaling law expected for a Gaussian coil distribution of chain conformations,[27] which was still in reasonable agreement with the data for the homopolymer only. Our new results thus emphasize the point made in ref 11 that "a larger range of molecular weights [was] required to obtain a reliable scaling coefficient".

The general trend of an increase of the intercluster distance in the monoionic, end-capped series is well understood. Given the fact that about the same number of chain ends aggregate to one cluster, as evidenced by the constant cluster size, the *volume* concentration of clusters should decrease linearly with molecular mass when assuming a constant density of the polymer microphase. If the spatial arrangement of the clusters remains the same, this would suggest scaling with an exponent $^1/_3$, which is in nice agreement with the experimental value of 0.334. This argument also suggests that the polymer chains connecting the clusters cannot assume the conformational distribution corresponding to a Gaussian coil. The fact that the data of the monoionic homopolymer and corresponding diblock copolymer can be fit by the same law within experimental error suggests that the ion clusters are evenly distributed within the poly(isoprene) microphase in the block copolymer rather than significantly repelled from the block copolymer interface.

In the zwitterionic series, the data can be discussed within a simple model of a two-dimensional distribution of the ion clusters in the interface between the microphases. As the number of block junctions and the average spatial requirements of a block junction in the interface do not depend on chain length, to a first approximation the interface area should be the same in all samples with a given morphology. As the number of clusters is also the same for a constant aggregation number, the *area* concentration of clusters should not depend on chain length. Assuming again that the spatial arrangement of the clusters remains the same, we find that also the intercluster distances should not depend on chain length, which is in agreement with our experimental result.

The time-domain DEER data for the samples μQ25, μS25, and μZ25 shown in Figure 6b exhibit a larger variation of curvature than the corresponding data for the homopolymers in ref 11. The center peak corresponding to the cluster size is most pronounced in μQ25, which indicates that the clusters of quaternary ammonium ions are better defined than the clusters containing sulfonate groups; see also Figure 6 of ref 11. For μQ25 we find a cluster size of 1.8 nm and an intercluster distance of 5.3 nm, which are not significantly different from sample Z24. Sample μS25 with a cluster size of 2.2 nm and an intercluster distance of 6.3 nm has the same topology as a monoionic sample in the α,ω series (see Figure 1), and the characteristic distances do indeed fit into this series. For μZ25 we could only determine the cluster size (1.8 nm); no second characteristic distance could be found in the distance distribution. This can be rationalized by considering the distribution of clusters in the interface of a bicontinuous structure. Such a distribution does not feature well-defined distances in space even if the distances in the curved interface are well-defined.

Conclusion

Variable temperature CW EPR measurements reveal a bimodal distribution of the rotational correlation times of ionic spin probes attached to ion clusters in μ,ω-macrozwitterionic and monoionic block copolymers if the ion clusters are situated in the block copolymer interface. The spectra can be analyzed semiquantitatively as superpositions of the spectra of a "slow" and "fast" component which can in turn be attributed to spin probes on the ion cluster surface exposed to the more rigid poly(styrene) and the more mobile poly(isoprene) microphase, respectively. In the case of the μ,ω-macrozwitterionic sample the fraction of cluster interface with poly(isoprene) is increased by a factor of 2 with respect to that of the monoionic species with a charge in the interface. DEER measurements show that there is no significant difference in the cluster size or intercluster distance for comparable block copolymers with ionic groups either at the block junction point or at the chain end. No defined intercluster distance could be detected for a μ,ω-macrozwitterionic ionomer with a cubic bicontinuous morphology. For α,ω-macrozwitterionic block copolymers, ion cluster sizes were also found to be independent of the molecular mass of the ionomers between about 10 and 50 kg mol^{-1} and to agree within experimental error with the corresponding monoionic species. For the α,ω-macrozwitterionic block copolymers also the intercluster distance does not depend on molecular mass M. This can be rationalized by a two-dimensional distribution of the clusters in the block copolymer interface of constant area. In monionic anionically end-labeled block copolymers the intercluster distance was found to scale roughly with $M^{1/3}$, which is the expected behavior if both the spatial arrangement and the polymer density are independent of the chain length.

Acknowledgment. Financial support by the DFG Schwerpunkt "Polyelektrolyte" is gratefully acknowledged.

References and Notes

(1) Barron, A. E.; Zuckermann, R. N. *Curr. Opin. Chem. Biol.* **1999**, *3*, 681.
(2) Sarikaya, M., Aksay, I. A., Eds.; *Biomimetics*; AIP Press: New York, 1995.
(3) Schlick, L., Ed.; *Ionomers: Characterization, Theory, and Applications*; CRC Press: New York, 1996.
(4) Eisenberg, A.; Kim, J.-S. *Introduction to Ionomers*; Wiley-Interscience: New York, 1998.
(5) Hashimoto, T.; Shibayama, M.; Kawai, H. *Macromolecules* **1980**, *13*, 1237.
(6) Bates, F. S. *Science* **1991**, *251*, 898.
(7) Hamley, I. W. *The Physics of Block Copolymers*; Oxford University Press: Oxford, 1998.
(8) Schädler, V.; Franck, A.; Wiesner, U.; Spiess, H. W. *Macromolecules* **1997**, *30*, 3832.
(9) Schädler, V.; Kniese, V.; Thurn-Albrecht, T.; Wiesner, U.; Spiess, H. W. *Macromolecules* **1998**, *31*, 4828.
(10) Schöps, M.; Leist, H.; DuChesne, A.; Wiesner, U. *Macromolecules* **1999**, *32*, 2806.
(11) Pannier, M.; Schädler, V.; Schöps, M.; Wiesner, U.; Jeschke, G.; Spiess, H. W. *Macromolecules* **2000**, *33*, 7812.

(12) Schädler, V.; Spickermann, J.; Räder, H. J.; Wiesner, U. *Macromolecules* **1996**, *29*, 4865.
(13) Schöps, M.; Junker, S.; Räder, H.-J.; Wiesner, U. *Macromol. Chem. Phys.*, submitted for publication.
(14) Pannier, M.; Veit, S.; Godt, A.; Jeschke, G.; Spiess, H. W. *J. Magn. Reson.* **2000**, *142*, 331.
(15) Schädler, V.; Wiesner, U. *Macromolecules* **1997**, *30*, 6698.
(16) Schöps, M. *Ladungen an definierten Stellen von Diblockcopolymeren: Struktur und Dynamik*; Tectum Edition Wissenschaft: Marburg, 2000.
(17) Hajduk, D. A.; Harper P. E.; Gruner, S. M.; Honeker, C. C.; Kim, G.; Thomas, E. L.; Fetters, L. J. *Macromolecules* **1994**, *27*, 4063.
(18) Rabold, G. P. *J. Polym. Sci., Part A-1* **1969**, *7*, 1203.
(19) Bullock, A. T.; Cameron, G. G.; Miles, I. S. *Polymer* **1976**, *23*, 1536.
(20) Hadjichristidis, N. *J. Polym. Sci., Part A* **1999**, *37*, 860.
(21) Eaton, G. R., Eaton, S. S., Berliner, L. J., Eds.; *Biological Magnetic Resonance*; Kluwer Publishing: Amsterdam, 2001; Vol. 19.
(22) Borbat, P. P.; Freed J. H. *Chem. Phys. Lett.* **1999**, *313*, 145.
(23) Milov, A. D.; Salikhov, K. M.; Shirov, M. D. *Fiz. Tverd. Tela (Leningrad)* **1981**, *23*, 975.
(24) Milov, A. D.; Maryasov, A. G.; Tsvetkov, Y. D. *Appl. Magn. Reson.* **1998**, *15*, 107.
(25) Martin, R. E.; Pannier, M.; Diederich, F.; Gramlich, V.; Hubrich, M.; Spiess, H. W. *Angew. Chem., Int. Ed. Engl.* **1998**, *37*, 2834.
(26) Jeschke, G.; Pannier, M.; Godt, A.; Spiess, H. W. *Chem. Phys. Lett.* **2000**, *331*, 243.
(27) Strobl, G. R. *The Physics of Polymers*; Springer-Verlag: Berlin, 1996.

MA010169C